Nano Research
DOI 10.1007/s12274-013-0344-4
Research Article
ISSN 1998-0124
CN 11-5974/O4

In situ Raman spectroscopy of topological insulator Bi_2Te_3 films with varying thickness

Chunxiao Wang[1,2], Xiegang Zhu[1], Louis Nilsson[3], Jing Wen[1], Guang Wang[1], Xinyan Shan[1], Qing Zhang[1], Shulin Zhang[2] (✉), Jinfeng Jia[1,4] (✉), and Qikun Xue[1]

[1] *State Key Laboratory for Low-Dimensional Quantum Physics, Department of Physics, Tsinghua University, Beijing 100084, China*
[2] *Department of Physics, Peking University, Beijing 100871, China*
[3] *Department of Physics and Astronomy and Interdisciplinary Nanoscience Center, Aarhus University, 8000 Aarhus C, Denmark*
[4] *Department of Physics, Shanghai Jiaotong University, Shanghai 200240, China*

Received: 28 April 2013
Revised: 18 June 2013
Accepted: 24 June 2013

KEYWORDS
topological insulator,
in situ Raman spectroscopy,
surface phonon mode,
thin film

ABSTRACT

Topological insulators (TIs) are a new state of quantum matter with a band gap in bulk and conducting surface states. In this work, the Raman spectra of topological insulator Bi_2Te_3 films prepared by molecular beam epitaxy (MBE) have been measured by an *in situ* ultrahigh vacuum (UHV)–MBE–Raman spectroscopy system. When the thickness of Bi_2Te_3 films decreases from 40 quintuple-layers (QL) to 1 QL, the spectral characteristics of some Raman modes appearing in bulk Bi_2Te_3 vary and a new vibrational mode appears, which has not been reported in previous studies and might be related to quantum size effects and symmetry breaking. In addition, an obvious change was observed at 3 QL when a Dirac cone formed. These results offer some new information about the novel quantum states of TIs.

1 Introduction

Topological insulators (TIs) are novel materials with a bulk insulating gap and gapless surface states. The gapless surface states are topologically protected by time reversal symmetry and described by the Dirac equation with zero mass [1, 2]. Bi_2Te_3, Bi_2Se_3, and Sb_2Te_3 are the most widely studied topological insulators [3], which have a single Dirac cone around the $\bar{\Gamma}$ point in the surface Brillouin zone (SBZ). The exotic topological and electromagnetic properties of TIs may lead to potential applications in spintronics and quantum computation [4].

Raman spectroscopy can be employed to investigate the composition, microstructure and internal motion states of various materials including nanostructures. Raman studies of the optical properties of TIs have been reported recently [5–10], and can be used to confirm the stoichiometry and crystal quality [11], whilst infrared-active modes are observed in nanoscale Bi_2Te_3 [5]. However, all the reported studies have been carried out in air. Although the topological properties

Address correspondence to Shulin Zhang, slzhang@pku.edu.cn; Jinfeng Jia, jfjia@sjtu.edu.cn

of TIs are stable in theory, the Fermi level is strongly modified [12] and the optical properties of such extreme thin films of several atomic layers might be very fragile under ambient conditions. Thus, for nanostructure materials prepared by the molecular beam epitaxy (MBE) technique, *in situ* measurements under ultrahigh vacuum (UHV) are highly desirable, since they can completely exclude the air-induced contamination and deterioration of materials and obtain true information about the sample. In this paper, we will present a Raman spectroscopy study of high quality Bi_2Te_3 films using a homebuilt *in situ* UHV-Raman spectral system coupled with MBE. *In situ* Raman spectroscopy experiments on Bi_2Te_3 films with thickness from 40 quintuple-layers (QL) to 1 QL were conducted. The experimental results show a new vibrational mode and its origin will be given.

2 Experimental

Bi_2Te_3 films were grown on clean Si (111)–7x7 substrates by MBE. Standard Knudsen diffusion cells were used to evaporate Bi (99.9999%) and Te (99.999%). The thickness of Bi_2Te_3 films was determined by scanning tunneling microscopy (STM) and reflected high energy electron diffraction (RHEED) [13].

Raman spectroscopic experiments were performed using a homebuilt system, shown schematically in Fig. 1. The electronic analysis (EA) chamber connected to the MBE setup was modifed so as to also be the sample chamber of the Raman spectral system. The laser incident and scattering light collecting optics were designed to match the sample in the EA chamber, in which the incident angle of the laser on the sample was set as a Brewster's angle. Such an arrangement allows the laser energy to be utilized to the greatest extent with, simultaneously, a high signal to noise ratio (SNR) of the Raman signal [14]. The spectrometer coupled to the MBE setup was a triple monochromator (Princeton Instrument TriVista 557) which has a high spectral resolution of about 1 cm^{-1} and extremely good stray light rejection in subtracted mode. This system ensures that the growth and spectral measurement of films are carried out under UHV conditions, which prevents the as-grown samples from contamination by the air and retains their intrinsic electronic properties.

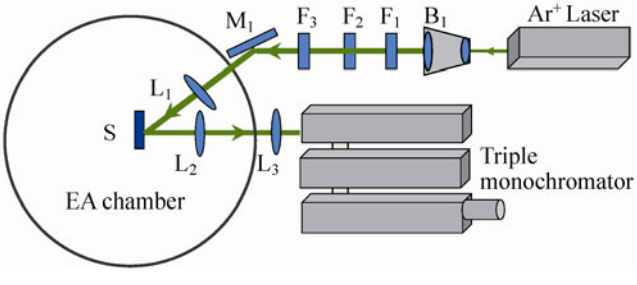

Figure 1 Schematic diagram of the *in situ* Raman spectroscopy system (B_1: Beam expander, F_1: Interference filter, F_2: Neutral density filter, F_3: Polarization rotator, M_1: Reflecting mirror, L_1: Focusing lens for incident light, S: Sample, L_2: Collector lens for scattering light, L_3: Focusing lens for scattering light, EA: Electronic analysis chamber).

3 Results and discussion

Single-crystal bulk Bi_2Te_3 belongs to the $D_{3d}^5(R\bar{3}m)$ space group with a rhombohedral crystal structure. The crystal exhibits a layered structure, with each layer consisting of five monoatomic planes of –Te(1)–Bi–Te(2)–Bi–Te(1)–, as is shown in Fig. 2(a). Each of these five atomic planes is referred to as a QL. As the primitive unit cell contains five atoms, there are 15 lattice vibration modes. At the Brillouin zone center ($q = 0$), the irreducible representations are $\Gamma = 2A_{1g} + 3A_{1u} + 2E_g + 3E_u$ [15]. Three of these modes are acoustic phonons, $A_{1u} + E_u$, and 12 are optical phonons, $2A_{1g} + 2A_{1u} + 2E_g + 2E_u$. There are four Raman active modes, E_g^1, A_{1g}^1, E_g^2, and A_{1g}^2, and their vibration patterns [16] are shown in Fig. 2(b). These four Raman active modes are expected at the wavenumbers 36.5, 62.0, 102.3, and 134.0 cm^{-1}, respectively.

The observed Raman spectra of Bi_2Te_3 films with thicknesses of 0.8 QL, 1 QL, 2 QL, 3 QL, 5 QL, 6 QL, 7 QL, and 40 QL are shown in Fig. 2(a). Figures 2(b) and 2(c) show the amplified Raman spectra of Bi_2Te_3 films with a thickness of 40 QL and 2 QL, respectively. The frequency and corresponding assignment of Raman peaks in Fig. 3 are listed in Table 1. In Fig. 3, besides the expected classical Raman active modes, there are some new vibration modes appearing. A new vibration mode at 95 cm^{-1} appears gradually as the film thickness decreases from 40 to 1 QL, as is shown in Table 1. This vibration mode can be interpreted as

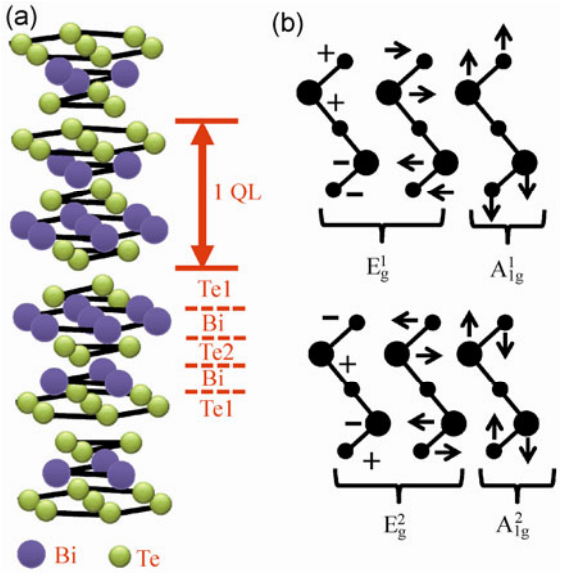

Figure 2 (a) Crystal structure of Bi_2Te_3; (b) Raman-active modes of Bi_2Te_3.

a surface phonon mode (SPM), which is only observed in nanosized materials. The decrease of the superficial force constant in nanosized crystals can lead to an increase in the interatomic distance in surface layers with respect to that in bulk samples. Thus, this surface phonon mode has a lower frequency than E_g^2, while both of them have similar behavior. Meanwhile, the frequency of this mode does not change with decreasing film thickness. The ratio of superficial atom number to bulk atom number increases as the sample size decreases (in our case, as sample thickness decreases), which will result in an increase in the Raman scattering intensity of the SPM relative to the adjacent normal Raman mode [14, 17]. For Bi_2Te_3 films, the intensity ratio of SPM to E_g^2 (I_{SPM}/I_{Eg}^2) increases as the film thickness decreases from 40 to 1 QL, as can be seen in Fig. 4(a). In Fig. 4(a), we can see that the full width at half maximum (FWHM) of the SPM broadens as the sample thickness decreases. Thin films (~QL) lead to relaxation of the Raman selection rules and make phonons with wave vectors in the range of $(q - \Delta q) — (q + \Delta q)$ Raman active, which leads to the broadening of the FWHM [14]. As the sample thickness decreases, the FWHM broadening effect becomes much more evident.

Some additional peaks that we denote P1, P2, P3, and P4 are also observed in our experiment. P3 is probably an infrared-active mode of the Bi_2Te_3 film, which is caused by a size effect [5]. P4 only appears in the Raman spectra of Bi_2Te_3 films with a thickness of

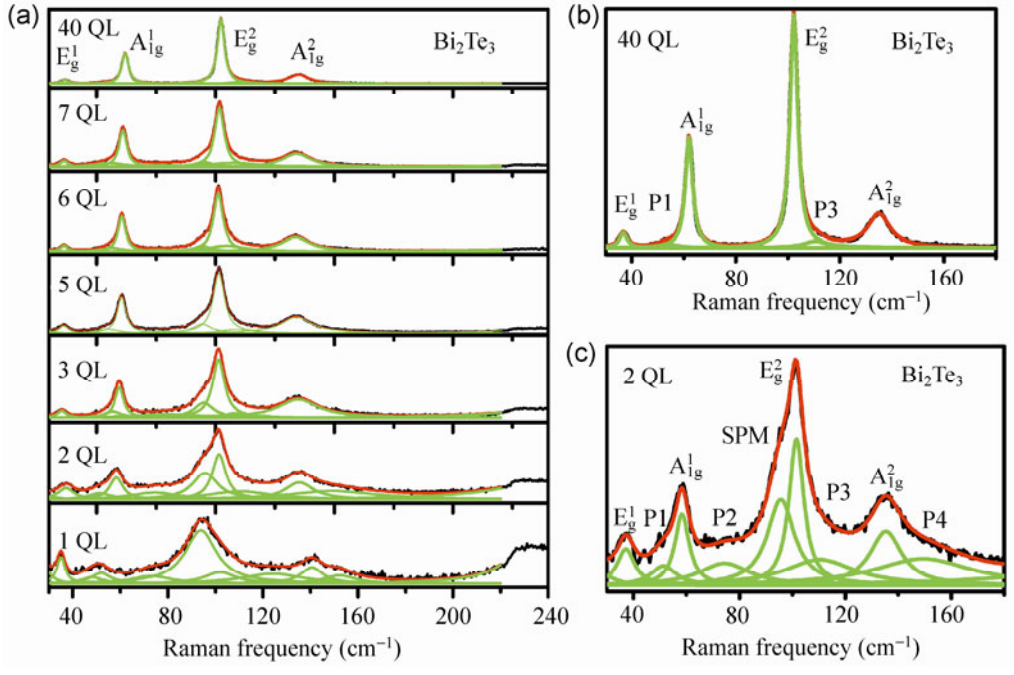

Figure 3 Observed Raman spectra of Bi_2Te_3 films with a thickness of 1 QL, 2 QL, 3 QL, 5 QL, 6 QL, 7 QL, and 40 QL (a), 40 QL (b), and 2 QL (c), where the green lines are the fitted spectra with Lorentzian lineshapes.

Table 1 Frequency and assignment of Raman peaks of Bi_2Te_3 films

	E_g^1	P1	A_{1g}^1	P2	SPM	E_g^2	P3	A_{1g}^2	P4
40 QL	37	54	62			102	111	135	
7 QL	36	55	61	78	95	102	108	134	
6 QL	36	56	61	76	94	101	105	134	
5 QL	36	55	61	79	95	102	109	134	
3 QL	35	57	60	80	95	101	109	135	
2 QL	37	51	58	74	96	102	110	135	149
1 QL	35	48	52	73	94	102	124	141	152
Bulk[a]	36.5		62.0			102.3		134.0	
40 QL[b]	38.9		61.3			101.3	116.2	133.0	

[a] Ref. [16]
[b] Ref. [5]

2 QL and 1 QL. This might be caused by quantum size effects and variation in band structure on going from 2D to 1D materials [18]. The origins of P1 and P2 are unknown and this needs further study. The broadened peak at 240 cm^{-1} is assigned to the longitudinal acoustic (LA) mode of the silicon substrate at 330 cm^{-1} [19, 20], and its intensity becomes higher as the Bi_2Te_3 film becomes thinner. Thus, the intensity of the LA mode offers circumstantial evidence of the variation in film thickness.

In Fig. 4(b), we can see that an obvious redshift (from 62 to 51.9 cm^{-1}) occurs for the A_{1g}^1 mode as the sample thickness decreases from 40 to several QL, especially to 1 QL. For the A_{1g}^2 mode, an obviously blueshift (from 134.1 to 140.6 cm^{-1}) occurs as the sample thickness decreases from 5 to 1 QL. It can be seen from Fig. 2 that Bi and Te atoms vibrate perpendicularly to the layer surface for both A_{1g}^1 and A_{1g}^2 modes. Therefore, decreasing the film thickness will have a significant effect on these two modes, thus inducing a frequency shift. The relative vibration directions for Bi and Te are different for A_{1g}^1 and A_{1g}^2, which leads to the respective redshift and blueshift of the Raman frequencies.

Based on the above discussion, we can see that there is dramatic change in the overall Raman scattering for Bi_2Te_3 films with a thickness less than 3 QL. This might be the result of phonon confinement effects which show a marked increase when the thickness is below the size of the unit cell (3 QL). On the other hand,

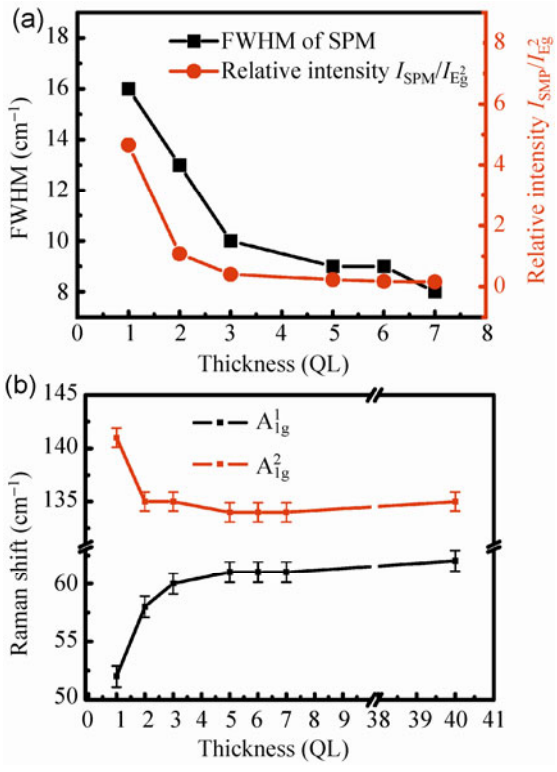

Figure 4 (a) FWHM of SPM and intensity ratio $I_{SPM}/I_{E_g^2}$ for Bi_2Te_3 films with different thickness. (b) Frequency variation of A_{1g}^1 and A_{1g}^2 as a function of film thickness.

a Dirac cone forms on the surface of Bi_2Te_3 films with a thickness above 2 QL, as has been demonstrated by angle-resolved photoemission spectroscopy (ARPES) [21]. Thus, there might be a relationship between the Raman spectra and the topological properties of Bi_2Te_3 films, which means that Raman scattering techniques might offer possibilities to probe the topological properties of TIs.

4 Conclusions

An *in situ* UHV–MBE–Raman spectroscopy system, which can completely exclude the air-induced contamination and deterioration of materials, has been successfully set up. Using this system, we performed *in situ* Raman spectroscopy on Bi_2Te_3 films with thicknesses from 40 to 1 QL. We found the frequencies of the A_{1g}^1 and A_{1g}^2 modes were respectively redshifted and blueshifted with decreasing film thickness. A surface phonon mode (SPM) is also observed, for which the FWHM broadens and the relative

intensity increases as the film thickness decreases. The formation of a Dirac cone can induce dramatic changes in the Raman scattering. The results obtained here provide some new information about the novel quantum states of topological insulators.

Acknowledgements

This work was supported by the Ministry of Science and Technology of the People's Republic of China (MOST) of China (973 Project, 2011CB922202 and 2009CB929403) and National Natural Science Foundation of China (NSFC) (Grant Nos. 91021002, 11227404, and 91221302).

References

[1] Qi, X. L.; Zhang, S. C. The quantum spin Hall effect and topological insulators. *Phys. Today* **2010**, *63*, 33–38.

[2] Moore, J. E. The birth of topological insulators. *Nature* **2010**, *464*, 194–198.

[3] Zhang, H. J.; Liu, C. X.; Qi, X. L.; Dai, X.; Fang, Z.; Zhang, S. C. Topological insulators in Bi_2Se_3, Bi_2Te_3, and Sb_2Te_3 with a single Dirac cone on the surface. *Nat. Phys*. **2009**, *5*, 438–442.

[4] Hasan, M. Z.; Kane, C. L. Colloquium: Topological insulators. *Rev. Mod. Phys*. **2010**, *82*, 3045–3067.

[5] Shahil, K. M. F.; Hossain, M. Z.; Teweldebrhan, D.; Balandin, A. A. Crystal symmetry breaking in few-quintuple Bi_2Te_3 films: Applications in nanometrology of topological insulators. *Appl. Phys. Lett.* **2010**, *96*, 153103.

[6] Zhang, J.; Peng, Z. P.; Soni, A.; Zhao, Y. Y.; Xiong, Y.; Peng, B.; Wang, J. B.; Dresselhaus, M. S.; Xiong, Q. H. Raman spectroscopy of few-quintuple layer topological insulator Bi_2Se_3 nanoplatelets. *Nano Lett.* **2011**, *11*, 2407–2414.

[7] Gnezdilov, V.; Pashkevich, Y. G.; Berger, H.; Pomjakushina, E.; Conder, K.; Lemmens, P. Helical fluctuations in the Raman response of the topological insulator Bi_2Se_3. *Phys. Rev. B* **2011**, *84*, 195118.

[8] Zhao, S. Y. F.; Beekman, C.; Sandilands, L. J.; Bashucky, J. E. J.; Kwok, D.; Lee, N.; LaForge, A. D.; Cheong, S. W.; Burch, K. S. Fabrication and characterization of topological insulator Bi_2Se_3 nanocrystals. *Appl. Phys. Lett.* **2011**, *98*, 141911.

[9] Dang, W. H.; Peng, H. L.; Li, H.; Wang, P.; Liu, Z. F. Epitaxial heterostructures of ultrathin topological insulator nanoplate and graphene. *Nano Lett.* **2010**, *10*, 2870–2876.

[10] Russo, V.; Bailini, A.; Zamboni, M.; Passoni, M.; Conti, C.; Casari, C. S.; Bassi, A. L.; Bottani, C. E. Raman spectroscopy of Bi–Te thin films. *J. Raman Spectrosc*. **2008**, 39, 205–210.

[11] Zhang, G. H.; Qin, H. J.; Teng, J.; Guo, J. D.; Guo, Q. L.; Dai, X.; Fang, Z.; Wu, K. H. Quintuple-layer epitaxy of thin films of topological insulator Bi_2Se_3. *Appl. Phys. Lett.* **2009**, *95*, 053114.

[12] Chen, C. Y.; He, S. L.; Weng, H. M.; Zhang, W. T.; Zhao, L.; Liu, H. Y.; Jia, X. W.; Mou, D. X.; Liu, S. Y.; He, J. F. et al. Robustness of topological order and formation of quantum well states in topological insulators exposed to ambient environment. *P. Natl. Acad. USA*. **2012**, *109*, 3694–3698.

[13] Wang, G.; Zhu, X. G.; Sun, Y. Y.; Li, Y. Y.; Zhang, T.; Wen, J.; Chen, X.; He, K.; Wang, L. L.; Ma, X. C. et al. Topological insulator thin films of Bi_2Te_3 with controlled electronic structure. *Adv. Mater.* **2011**, *23*, 2929–2932.

[14] Zhang, S. L. *Raman Spectroscopy and its Application in Nanostructures*; Wiley: Chichester, 2012.

[15] Richter, W.; Becker, C. R. A Raman and far-infrared investigation of phonons in the rhombohedral V_2-VI_3 compounds Bi_2Te_3, Bi_2Se_3, Sb_2Te_3, and $Bi_2(Te_{1-x}Se_x)_3$ $(0 < x < 1)$, $(Bi_{1-y}Sb_y)_2Te_3$ $(0 < y < 1)$. *Phys. Stat. Sol. (b)* **1977**, *84*, 619–628.

[16] Kullmann, W.; Geurts, J.; Richter, W.; Lehner, N.; Rauh, H.; Steigenberger, U.; Eichhorn, G.; Geick, R. Effect of hydrostatic and uniaxial pressure on structural properties and Raman active lattice vibrations in Bi_2Te_3. *Phys. Stat. Sol. (b)* **1984**, *125*, 131–138.

[17] Zuo, J.; Xu, C. Y.; Liu, X. M.; Wang, C. S.; Wang, C. Y.; Hu, Y.; Qian, Y. T. Study of the Raman spectrum of nanometer SnO_2. *J. Appl. Phys.* **1994**, *75*, 1835–1836.

[18] Zhang, W.; Yu, R.; Zhang, H.; Dai, X.; Fang, Z. First principles studies on 3-dimentional strong topological insulators: Bi_2Te_3, Bi_2Se_3, and Sb_2Te_3. *New J. Phys.* **2010**, *12*, 65013–65020.

[19] Dolling, G. *Inelastic Scattering Neutrons in Solids and Liquids*; IAEA: Vienna, 1963; 2, pp37.

[20] Tubino, R.; Piseri, L.; Zerbi, G. Lattice dynamics and spectroscopic properties by a valence force potential of diamondlike crystals: C, Si, Ge, and Sn. *J. Chem. Phys*. **1972**, *56*, 1022–1039.

[21] Li, Y. Y.; Wang, G.; Zhu, X. G.; Liu, M. H.; Ye, C.; Chen, X.; Wang, Y. Y.; He, K.; Wang, L. L.; Ma, X. C. et al. Intrinsic topological insulator Bi_2Te_3 thin films on Si and their thickness limit. *Adv. Mater.* **2010**, *22*, 4002–4007.